Cumhuriyet Science Journal
CSJ

e-ISSN: 2587-246X
ISSN: 2587-2680

Cumhuriyet Sci. J., Vol.39-2(2018) 406-412

# Influence of Gd Substitution on Structural, Magnetic and Magnetocaloric Properties in $(La_{0.8}Gd_{0.2})_{0.85}Ag_{0.15}MnO_3$ Perovskite Manganite System

***Ahmet EKICIBIL[1*], Ali Osman AYAS[2], Mustafa AKYOL[3]***

[1]*Çukurova University, Department of Physics, Adana, TURKEY*

[2]*Adıyaman University, Department of Mechatronics Engineering, Adıyaman, TURKEY*

[3]*Adana Science and Technology University, Department of Materials Engineering, Adana, TURKEY*

Received: 02.02.2018; Accepted: 30.04.2018 *http://dx.doi.org/10.17776/csj.388985*

**Abstract:** In this paper, the effect of Gd substitution with La on structural, magnetic and magnetocaloric properties in $(La_{0.8}Gd_{0.2})_{0.85}Ag_{0.15}MnO_3$ manganite sample prepared by sol-gel method has been studied. The crystal properties have been investigated by x-ray diffraction technique that shows the sample is in rhombohedral structure with $R\bar{3}c$ space group. In addition to this structure, small amount of reflections belongs to $GdMn_2O_5$ phase is detected. Scanning electron microscope images show that the sample is constituted from square shaped grains. Energy dispersive x-ray spectroscopy analysis shows that the sample includes all expected elements. The sample exhibits magnetic phase transition from ferromagnetic to paramagnetic phase at around 149 K temperature. Applied field dependence of magnetization under isothermal process *M(H)* shows that the nature of the phase transition is second order and maximum magnetic entropy change ($-\Delta S_M$) value calculated from *M(H)* curves is found as 1.73 J/kgK under 50 kOe external magnetic field change.

***Keywords*:** Perovskites, magnetic cooling, magnetocaloric effect, magnetic entropy change.

# $(La_{0.8}Gd_{0.2})_{0.85}Ag_{0.15}MnO_3$ Perovskit Manganit Sisteminde Gd Yer Değiştirmesinin Yapısal Manyetik ve Manyetokalorik Özellikleri Üzerine Etkisi

**Özet:** Bu makalede, sol-jel yöntemi ile hazırlanan $(La_{0.8}Gd_{0.2})_{0.85}Ag_{0.15}MnO_3$ sisteminde Gd ile La yer değiştirmesinin yapısal, manyetik ve manyetokalorik etkileri çalışılmıştır. Kristal yapı X-Işınları kırınım tekniği ile araştırılmıştır ve bu teknik örneğin $R\bar{3}c$ uzay grubunda rombohedral yapıda olduğunu göstermiştir. Bu yapının yanında $GdMn_2O_5$ yapısına ait çok küçük miktarda safsızlık fazına ait yansımalar da tespit edilmiştir. Taramalı Elektron Mikroskobu fotoğrafları örneğin kare yapılı taneciklerden oluştuğunu göstermektedir. X-ışınları spektroskopisi analizleri ise örneğin tüm beklenen elementleri içerdiğini göstermiştir. Sıcaklığa bağlı mıknatıslanma, *M(T)*, ölçümleri sıcaklığın artışıyla örneğin 149 K sıcaklıkta ferromanyetik fazdan paramanyetik faza doğru bir manyetik faz geçişi sergilediğini göstermiştir. İzotermal şartlarda yapılan, uygulanan alana bağlı mıknatıslanma, *M(H)*, ölçümleri faz geçişinin doğasının ikinci dereceden olduğunu göstermiştir ve *M(H)* verisinden maksimum manyetik entropi değişim değeri, ($-\Delta S_M$), 50 kOe dış manyetik alan değişimi altında, 1.73 J/kgK olarak hesaplanmıştır.

***Anahtar Kelimeler*:** Perovskitler, manyetik soğutma, manyetokalorik etki, manyetik entropi değişimi.

* Corresponding author. *Email address:* *ahmetcan@cu.edu.tr*
http://dergipark.gov.tr/csj ©2016 Faculty of Science, Cumhuriyet University

## 1. INTRODUCTION

Magnetic Cooling (MC) technology offers more energy efficiency rate than existed cooling technology. Additionally, MC uses environmentally friendly technology [1-3]. Due to these advantages, in recent years, many researchers focus on this technology. Magnetic cooling technology mainly based on a term which is called as magnetocaloric effect. This phenomena is a property that arises from coupling of magnetic sub-lattice by applied magnetic field. Increasing applied magnetic field yields aligning magnetic moments with the direction of applied magnetic fields and decreases magnetic entropy of the system. If this situation occurs under adiabatic conditions, lattice and electronic entropy of the system increase to keep total entropy constant and temperature of the system increases. When applied magnetic field is removed, the spin system behaves inversely and the temperature of the system decreases. Thus, this kind of cooling is called MC.

MC community works on wide range of material families to find optimized magnetic cooling materials such as manganites [4-7], La-Fe-Si alloys [7] Gd based materials [7], etc. Among them, $ABO_3$ type manganite compounds attract interests because of having good properties for applications such as low cost, easy elaboration, possible tunable Curie temperature ($T_C$) and high chemical stability [8]. Ferromagnetic double-exchange, antiferromagnetic super-exchange and spin phonon coupling properties are major factors that affect the magnetocaloric properties in manganites [9-12]. These interactions can be determined from the parameters like mismatch effect [13], oxygen stoichiometry [14], average A site ionic size [15] and doping level [16]. In recent years, La site substitution with various 1+ and 2+ cations have been worked to understand the effect of substitution on the properties given above (5,8) [8]. However, the effect of substitution with 3+ cations has not been explained in detail yet [8]. Therefore, in this study, the effect of $Gd^{3+}$ substitution with $La^{3+}$ on structural, magnetic and magnetocaloric properties is studied in $(La_{0.8}Gd_{0.2})_{0.85}Ag_{0.15}MnO_3$ manganite sample.

## 2. EXPERIMENTAL PROCEDURE

The polycrystalline $(La_{0.8}Gd_{0.2})_{0.85}Ag_{0.15}MnO_3$ sample labelled as LGAM-2 has been synthesized via sol-gel method by using high purity (≥99.99 %) $La_2O_3$, $Mn(NO_3)_2{\cdot}4H_2O$, $Gd(NO_3)_3{\cdot}6H_2O$, $AgNO_3$ powders as starting materials. Mono ethylene glycol (99.9% purity), citric acid monohydrate (99.9% purity), hydrochloric acid (37% purity) and nitric acid (70% purity) were used as a chelating substance. Details of the sample preparation process were explained in our previous work [17]. Powder X-Ray Diffraction (XRD) pattern of the sample has been measured by SIEMENS D5000 diffractometer with Cu-$K_\alpha$ radiation at room temperature. The analysis of XRD pattern was carried out by the Fullprof software based on the Rietveld method and X'Pert High score Plus software. The image of grain structure was taken via ZEISS EVO-40 Scanning Electron Microscope (SEM), the morphological and compositional properties were investigated by Energy–Dispersive X-ray Spectroscopy (EDS). The temperature and magnetic field dependences of the magnetization, *M(T)* and *M(H)*, were investigated by using a Quantum Design – Physical Properties Measurement System (PPMS) with Vibrating Sample Magnetometer (VSM) module. The *M(T)* was performed by sweeping temperature from 10 to 350 K under both Zero-Field Cooled (ZFC) and Field Cooled (FC) process. In ZFC process, the sample was cooled dawn to 10 K without applied magnetic field. Then, a small magnetic field (250 Oe) was applied to the sample. After that, magnetization was measured by sweeping temperature from 10 to 350 K. In FC process, magnetization was measured under a magnetic field of 250 Oe during cooling from 350 to 10 K.

## 3. RESULTS and DISCUSSIONS

The structure of the powdered sample is characterized by XRD technique. XRD data is analyzed with Rietveld refinement by using Fullprof software.

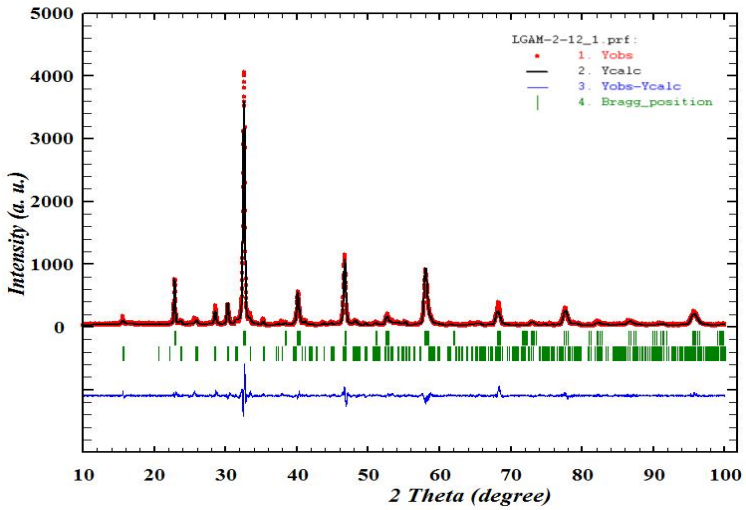


**Figure 1.** XRD pattern of the $(La_{0.8}Gd_{0.2})_{0.85}Ag_{0.15}MnO_3$ manganite sample observed from Rietveld refinement is showing orthorhombic symmetry. Red asterisks, black line, green ticks in first line and green ticks in second line indicate observed, calculated data, main phase and impurity phase, respectively.

The XRD pattern of the sample is shown in Fig. 1 that indicates polycrystalline behavior. According to the refinement, main structure of the sample is indexed as rhombohedral phase with $R\bar{3}c$ space group. In addition to the main characteristic of the structure, small reflection which is indexed as $GdMn_2O_5$ with Pbam space group is detected. Due to the non-ferromagnetic nature of the $REMn_2O_5$ (RE: Rare Earth) structure[18], it could be said that impurity phase doesn't affect the magnetocaloric behavior of the sample. The crystal structure found from Rietveld refinement is schematically illustrated at various axes in Fig. 2.

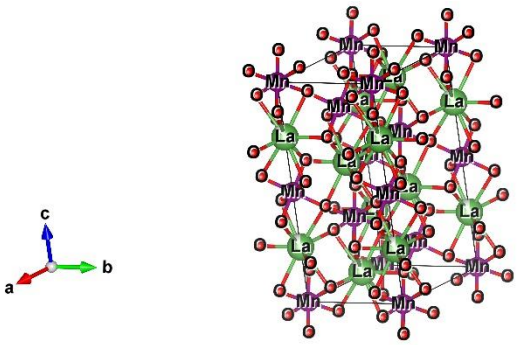


**Figure 2.** Crystal structure of the $(La_{0.8}Gd_{0.2})_{0.85}Ag_{0.15}MnO_3$ sample that constituted from $MnO_6$ octahedrals.

The lattice parameters, unit cell volume, Mn-O bond distance, Mn-O-Mn bond angle, average *A* site average ionic radius and mismatch coefficient are tabulated in Table 1 for LGAM-2 sample.

**Table 1.** Unit cell parameters, unit cell volume *V*, average *A* site ionic radius $r_A$, mismatch effect coefficient $\sigma^2$, Mn-O bond distance, Mn-O-Mn bond angle for $(La_{0.8}Gd_{0.2})_{0.85}Ag_{0.15}MnO_3$ sample.

| Properties | LGAM-2 |
|---|---|
| **a = b (Å)** | 5.5075 |
| **c (Å)** | 13.4014 |
| **V (Å$^3$)** | 352.0319 |
| **$r_A$ (Å)** | 0.1171 |
| **$\sigma^2$ (Å$^2$)** | 0.00261 |
| **Mn-O bond distance (Å)** | 4.3395 |
| **Mn-O-Mn bond angle (θ)** | 159.83537 |

It can be seen from the Table 1 that lattice parameters are in accordance with the values given in the literature [4, 8, 17]. (4,8,17) To find out relation between structural and magnetic properties, we have tried to calculate average A site ionic radius $r_A$, mismatch effect coefficient $\sigma^2$ parameters of the sample. This situation arises from the smaller ionic radius of Gd than La [19]. Substitution of an element with smaller ionic radius element yields to decrease average A site ionic radius, $r_A$, [5] and in this work, decreasing $r_A$ also supports this situation. Decreasing $r_A$ yields to

increase mismatch effect $\sigma^2$ [5] calculated from Eq.1 as in this case exhibited in Table 1.

$$\sigma^2 = \Sigma_i x_i r_i^2 - \langle r_A \rangle^2 \quad (1)$$

Decreasing $r_A$ and increasing $\sigma^2$ yield to tilt of $MnO_6$ octahedra.

In order to perform the surface morphology and the compositional properties of the sample, SEM imaging and EDS spectroscopy techniques have been carried out. The result is exhibited in Fig. 3. It is clear from the SEM image that the sample is constituted of square shaped grains of which boundaries are evident. Additionally, twiggy like structures are also detected in the SEM images. This twiggy like structures indicate $GdMn_2O_5$ crystals detected in XRD analysis. EDS spectra of the sample shows that all expected elements are recognized. There is no removal of prepared elements during calcination and sintering treatments, and there is no impurity elements detected with in the sensitivity limits of the measurement.

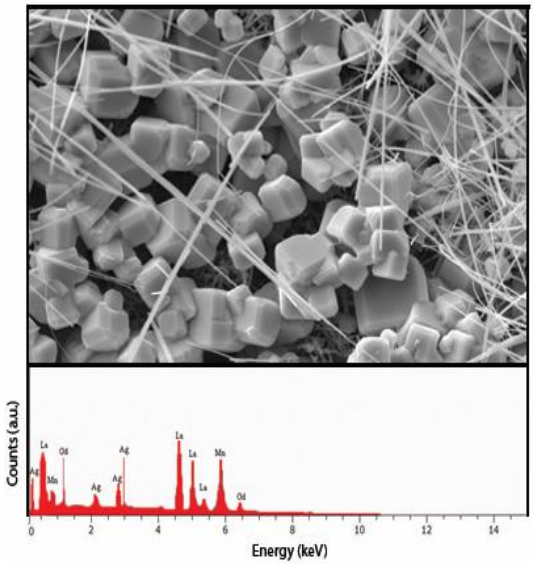


**Figure 3.** SEM image and EDS spectrum of the $(La_{0.8}Gd_{0.2})_{0.85}Ag_{0.15}MnO_3$ sample.

The temperature dependence of magnetization *M(T)* has been used to determine the magnetic phase transition temperature of the sample. *M(T)* measurement has been performed in two modes which are field cooled (FC) and zero-field cooled (ZFC) by sweeping temperature in the range from 10 to 350 K in applied magnetic field of 250 Oe. The result of the *M(T)* is shown in Fig. 4.

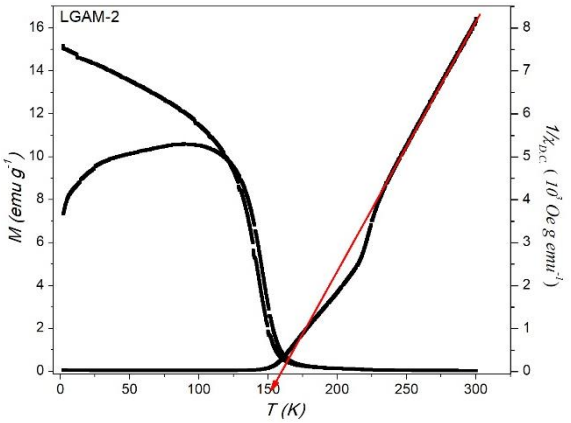


**Figure 4.** Temperature dependence of magnetization for $(La_{0.8}Gd_{0.2})_{0.85}Ag_{0.15}MnO_3$ sample Left axes: under FC and ZFC mode magnetization. Right Axes: inverse susceptibility versus temperature graph.

From the Fig. 4, for FC mode, it can be seen that the magnetization of the sample slowly decreases by increasing temperature, and then it sharply decreases around the magnetic phase transition temperature, $T_C$. The ZFC curve behaves similarly with FC curve at high temperatures, but it starts to lie lower at low temperatures. This difference can be attributed to magnetic anisotropy and domain wall pinning effect of the sample. These facts also affect the behavior of the inverse susceptibility curve. Nonlinear behavior of this curve around paramagnetic side also indicates the presence of the magnetic anisotropy and domain wall pinning effect for the sample. While cooling a magnetic material through $T_C$, subjecting two different processes like applying magnetic field or not, leads to different spin arrangement that gives rise to different net magnetizations. If material includes non-ferromagnetic inhomogeneities with in the magnetic domain wall and/or crystallite boundaries, this difference of FC-ZFC magnetization increases which leads to increase the domain pinning effect [20]. $T_C$ value of the sample is determined by two methods. In the first way, the point where ZFC and FC mode split from each other can be determine as $T_C$. In the second way, $T_C$ is determined by extrapolation of the linearly

increased part of inverse susceptibility graph as shown in right axes of the Fig. 4. The intersection of the temperature axes and extrapolation line indicate the $T_C$ value of the sample. The $T_C$ value of the sample is determined from these two different methods and tabulated in Table 2.

It can be seen from Table 2 that $T_C$ is determined as 149 K. From the value obtained in the literature [5], the $T_C$ decreases from 260 K to 149 K by substitution of La with Gd. This decreasing in $T_C$ can be explained in terms of decreasing $r_A$, and increasing $\sigma^2$ values given in Table 1. Decreasing in $r_A$ yields to decrease of Mn-O bond distance, detract the Mn-O-Mn angle from the 180º that tilts the MnO6 octahedral as shown in Fig. 2. This tilting additionally leads to increase vibration movement of the $MnO_6$ octahedrals [5]. This tilting and vibration limit the movement of mobility electrons and this leads weakening the Double Exchange (DE) interaction of the sample. Additionally, increasing $\sigma^2$ (mismatch effect) also leads to decrease the mobility of the $e_g$ electrons and decrease the DE interaction of the sample. Decreasing DE interaction gives rise to weaking of ferromagnetism of the sample, so that $T_C$ value of the sample decreases.

**Table 2.** Curie temperature $T_C$, maximum magnetic entropy change $\Delta S_M$, for LGAM-2: $(La_{0.8}Gd_{0.2})_{0.85}Ag_{0.15}MnO_3$ sample.

| Sample | ΔH | LGAM-2 |
|---|---|---|
| $T_C$ (K) | - | 149 |
| | 10 kOe | 0.40 |
| | 20 kOe | 0.76 |
| $-\Delta S_M$ (J kg$^{-1}$K$^{-1}$) | 30 kOe | 1.15 |
| | 40 kOe | 1.45 |
| | 50 kOe | 1.73 |

Figure 5 shows the isothermal magnetization curves versus applied magnetic field up to 50 kOe at various temperatures between 96 and 198 K by 4 K steps for LGAM-2 sample.

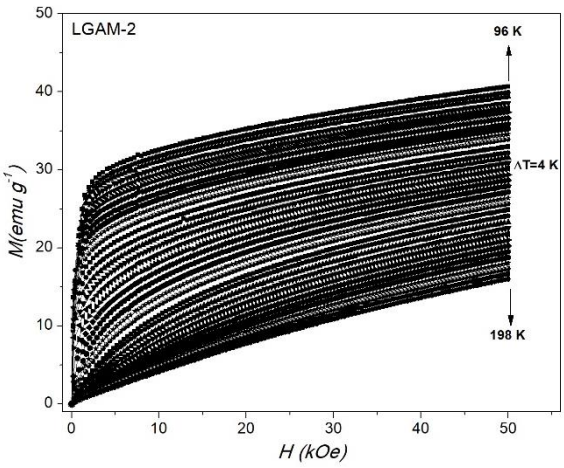


**Figure 5.** Isothermal magnetization curves of the $(La_{0.8}Gd_{0.2})_{0.85}Ag_{0.15}MnO_3$ sample.

It can be seen from the Fig.5 that sample shows, below $T_C$, typical ferromagnetic behavior by rapid increasing magnetization with increasing applied magnetic field and approach the saturation at higher fields. The curves start to increase linearly for higher temperatures and this situation indicates that the sample became paramagnetically ordered.

The magnetic entropy change, $(\Delta S_M)$ is calculated from experimental data. In accordance with the thermodynamic theory, the $\Delta S_M$ is given by,

$$\Delta S_M = S_M(T,H) - S_M(T,0) = \int_0^H \left(\frac{\partial S}{\partial H}\right)_T dH. \quad (2)$$

From the Maxwell's thermodynamic relation,

$$\left(\frac{\partial M}{\partial T}\right)_H = \left(\frac{\partial S}{\partial H}\right)_T. \quad (3)$$

Following expression can be obtained:

$$\Delta S_M = \int_0^H \left(\frac{\partial M}{\partial T}\right)_H dT. \quad (4)$$

Considering the discrete data obtained from the experimental measurements, following approximation of the integral can be employed to the Eq. (5).

$$\Delta S_M = \sum_i \frac{M_i - M_{i+1}}{T_{i+1} - T_i} \Delta H_i. \quad (5)$$

$\Delta S_M$ values of the sample are determined from the isothermal magnetization curves by using Eq. (5). Obtained $\Delta S_M$ values are tabulated in Table 2 and also shown in Fig. 6.

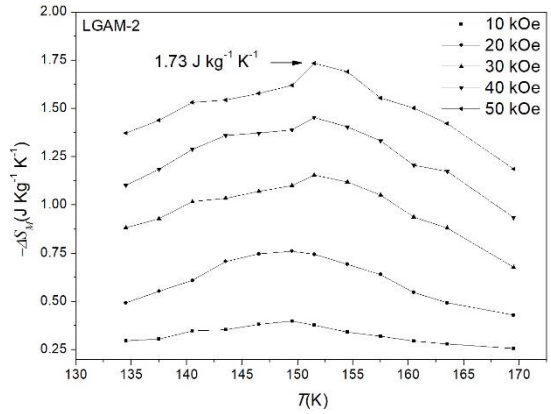


**Figure 6.** $\Delta S_M$ (T) for the $(La_{0.8}Gd_{0.2})_{0.85}Ag_{0.15}MnO_3$ sample.

The $-\Delta S_{M,max}$ values were found as 0.40, 0.76, 1.15, 1.45 and 1.73 J/kgK under applied magnetic fields of 10, 20, 30, 40 and 50 kOe, respectively. It can be also seen from the Table 2 that although the magnitude of $\Delta S_{M,max}$ values is comparable with some perovskites manganites reported in literature, it can be said that Gd substitution adversely affect the $\Delta S_M$ values and limits the practicable usage of the sample.

## 4. CONCLUSIONS

As a summary, the effect of substitution of La with Gd on structural, magnetic and magnetocaloric properties in $(La_{0.8}Gd_{0.2})_{0.85}Ag_{0.15}MnO_3$ manganite sample prepared by sol-gel method has been studied in detail. XRD results show that the sample crystallizes in rhombohedral structure with $R\bar{3}c$ space group and small amount of impurity is detected as $GdMn_2O_5$ phase. The SEM analysis show that the grains are square shape, their magnitudes are non-homogeneously distributed. The EDS spectra shows that sample includes all expected elements, there is no any impurity elements in the matrix. Sample shows magnetic phase transition from ferromagnetic to paramagnetic phase at $T_C$ which is determined as ~149 K. Maximum magnetic entropy change value is determined as 1.73 J/kgK. All these results show that substitution of La with Gd in $(La_{1-x}Gd_x)_{0.85}Ag_{0.15}MnO_3$ sample for x = 0.2 adversely affects the magnetocaloric properties.

## REFERENCES

[1] Gschneidner K.A., Pecharsky V.K. Rare Earths and Magnetic Refrigeration, Journal of Rare Earths, 24 (2006) 641-647.

[2] Gschneidner K.A., Pecharsky V.K., Pecharsky A.O.,Zimm C.B. Recent developments in magnetic refrigeration, in Rare Earths (1999), Woodward, R. C., Ed., 5: 69-73.

[3] Tishin A.M., Derkach A.V., Spichkin Y.I., et al., Magnetocaloric effect near a second-order magnetic phase transition, Journal of Magnetism and Magnetic Materials, 310 (2007) 2800.

[4] Ayaş A.O., Akyol M., Çetin S.K., Akça G., Ekicibil A., Özçelik B., Magnetocaloric Properties of La0. 85Ag0. 15MnO3 and (La0. 80Pr0. 20) 0.85 Ag0. 15MnO3 Compounds, Journal of Superconductivity and Novel Magnetism, 28 (2015) 1649.

[5] Ayaş A.O., Akyol M., Ekicibil A., Structural and magnetic properties with large reversible magnetocaloric effect in 0.85 Ag0. 15MnO3 compounds, Philosophical Magazine, 96 (2016) 922.

[6] Kılıç Çetin S., Acet M., Güneş M., Ekicibil A., Farle M., Magnetocaloric effect in (La1−xSmx)0.67Pb0.33MnO3 ($0 \leq x \leq 0.3$) manganites near room temperature, Journal of Alloys and Compounds, 650 (2015) 285.

[7] Tishin A.M., Magnetocaloric effect: Current situation and future trends, Journal of Magnetism and Magnetic Materials, 316 (2007) 351.

[8] Phan M.-H., Yu S.-C., Review of the magnetocaloric effect in manganite materials, Journal of Magnetism and Magnetic Materials, 308 (2007) 325.

[9] Zener C., Interaction between the d-Shells in the Transition Metals. II. Ferromagnetic Compounds of Manganese with Perovskite Structure, Physical Review, 82 (1951) 403.

[10] Millis A.J., Littlewood P.B., Shraiman B.I., Double Exchange Alone Does Not Explain the Resistivity of $La_{1-x}Sr_xMnO_3$, Physical Review Letters, 74 (1995) 5144.

[11] Goodenough J.B., Wold A., Arnott R.J., Menyuk N., Relationship Between Crystal Symmetry and Magnetic Properties of Ionic Compounds Containing Mn3+, Physical Review, 124 (1961) 373.

[12] Selmi A., M'Nassri R., Cheikhrouhou-Koubaa W., Boudjada N.C., Cheikhrouhou A., Effects of partial Mn-substitution on magnetic and magnetocaloric properties in $Pr_{0.7}Ca_{0.3}Mn_{0.95}X_{0.05}O_3$ (Cr, Ni, Co and Fe) manganites, Journal of Alloys and Compounds, 619 (2015) 627.

[13] Hao C., Zhao B., Huang Y., Kuang G., Sun Y., A-site-disorder-dependent magnetocaloric properties in the mono-valent-metal doped $La_{0.7}Ca_{0.3}MnO_3$ manganites, Journal of Alloys and Compounds, 509 (2011) 5877.

[14] M'nassri R., Cheikhrouhou A., Evolution of Magnetocaloric Behavior in Oxygen Deficient $La_{2/3}Ba_{1/3}MnO_{3-\delta}$ Manganites, Journal of Superconductivity and Novel Magnetism, 27 (2014) 1463.

[15] M'nassri R., Cheikhrouhou-Koubaa W., Koubaa M., Cheikhrouhou A., Effect of strontium substitution on the physical properties of Nd 0.5 Ca 0.5−x Sr x MnO 3 ($0.0 \leq x \leq 0.5$) manganites, IOP Conference Series: Materials Science and Engineering, 28 (2012) 012050.

[16] M'nassri R., Cheikhrouhou-Koubaa W., Boudjada N., Cheikhrouhou A., Magnetocaloric Effects in $Pr_{0.6-x}Er_xSr_{0.4}MnO_3$ ($0.0 \leq x \leq 0.2$) Manganese Oxides, Journal of Superconductivity and Novel Magnetism, 26 (2013) 1429.

[17] Ayaş A.O., Akyol M., Kılıç Çetin S., et al., Room temperature magnetocaloric effect in Pr1.75Sr1.25Mn2O7 double-layered perovskite manganite system, Philosophical Magazine, (2017) 1.

[18] Muñoz A., Alonso J.A., Martínez-Lope M.J., Pomjakushin V., André G., On the magnetic structure of PrMn 2 O 5 : a neutron diffraction study, Journal of Physics: Condensed Matter, 24 (2012) 076003.

[19] Shannon R.D., Revised effective ionic radii and systematic studies of interatomic distances in halides and chalcogenides, Acta Crystallographica Section A, 32 (1976) 751.

[20] Taşarkuyu E., Coşkun A., Irmak A.E., et al., Effect of high temperature sintering on the structural and the magnetic properties of $La_{1.4}Ca_{1.6}Mn_2O_7$, Journal of Alloys and Compounds, 509 (2011) 3717.